Title

Energy dissipation analysis of elastic–plastic materials

Authors

Yang, Han
Sinha, Sumeet Kumar
Feng, Yuan
et al.

Publication Date

2018-04-01

DOI

10.1016/j.cma.2017.11.009

Peer reviewed

Energy dissipation analysis of elastic–plastic materials

Han Yang[a], Sumeet Kumar, Sinha[a], Yuan Feng[a], David B. McCallen[b], Boris Jeremić[ab]

Abstract

Presented is an energy dissipation analysis framework for granular material that is based on thermodynamics. Theoretical formulations are derived from the second law of thermodynamics, in conjunction with a few plausible assumptions on energy transformation and dissipation. The role of plastic free energy is emphasized by a conceptual experiment showing its physical nature. Theoretical formulation is adapted in order to be applied in elastic–plastic finite element method (FEM) simulations. Developed methodology is verified through comparison of input work, stored energy, and energy dissipation of the system. Separation of plastic work into plastic free energy and energy dissipation removes a common mistake, made in a number of publications, where energy dissipation can attain negative values (energy production) which is impossible.

Keywords: Seismic energy dissipation, FEM, Computational geomechanics, Thermodynamics, Elastic–plastic materials, Plastic free energy

1. Introduction

Energy dissipation in elastic plastic solids and structures is the result of an irreversible dissipative process in which energy is transformed from one form to another and entropy is produced. The transformation and dissipation of energy is related to permanent deformation and damage within an elastic–plastic material. Of particular interest here is the dissipation of mechanical energy that is input into elastic–plastic solids by static or dynamic excitations.

Early work on plastic dissipation was done by Farren and Taylor [1] and Taylor and Quinney [2]. They performed experiments on metals and proved that a large part, but not all, of the input mechanical energy is converted into heat. The remaining part of the non-recoverable plastic work is known as the stored energy of cold work. The ratio of plastic work converted into heating (Quinney–Taylor coefficient), usually denoted as β, has been used in most later work on this topic. Based on large amount of experimental data, this ratio was determined to be a constant between 0.6 to 1.0 [[3], [4], [5], [6], [7], [8]].

More recently Rittel [[9], [10], [11]] published several insightful papers on the energy dissipation (heat generation) of polymers during cyclic loading, presenting both experimental and theoretical works. Rosakis et al. [12] presented a constitutive model for metals based on thermoplasticity that is able to calculate the evolution of energy dissipation. Follow up papers [[13], [14]] present assumptions to simplify the problem. One direct application of plastic dissipation to geotechnical engineering is presented by

Veveakis et al. [[15], [16]], using thermoporomechanics to model the heating and pore pressure increase in large landslides, like the 1963 Vajont slide in Italy.

In the past few decades, extensive studies have been conducted on energy dissipation in structures and foundations. Work by Uang and Bertero [17] has been considered a source and a reference for many recent publications dealing with energy as a measure of structural demand. Uang and Bertero [17] developed an energy analysis methodology based on absolute input energy (or energy demand). Numerical analysis results were compared with experiments on a multi-story building. In work by [17], hysteretic energy is calculated indirectly by taking the difference of absorbed energy and elastic strain energy. The term absorbed energy of each time step is simply defined as restoring force times incremental displacement. It is also stated that hysteretic energy is irrecoverable, which indicates that this parameter was considered the same as hysteretic dissipation or plastic dissipation. An equation for energy balance, is given by (Uang and Bertero [17]) as:

$$E_i = E_k + E_\xi + E_a = E_k + E_\xi + E_s + E_h \qquad (1)$$

where Ei is the (absolute) input energy, Ek is the (absolute) kinetic energy, Eξ is the viscous damping energy, Ea is the absorbed energy, which is composed of elastic strain energy Esand hysteretic energy Eh.

The problem with this approach is the absence of plastic free energy, which is necessary to correctly evaluate energy dissipation of elastic–plastic materials and to uphold the second law of thermodynamics. While there is no direct plot of plastic dissipation (hysteretic energy) in [17], since it was not defined directly, there are plots of other energy components. Plastic dissipation can be easily calculated from these plots. After doing this, indications of negative incremental energy dissipation, which violates the basic principles of thermodynamics, were found in various sections of the paper.

This misconception could be clarified by renaming hysteretic energy as plastic work, a sum of plastic dissipation and plastic free energy. Both plastic work and plastic free energy can be incrementally negative, but plastic dissipation (defined as the difference of plastic work and plastic free energy) must be incrementally non-negative during any time period. Unfortunately, this misconception has been inherited (if not magnified) by many following studies on energy analysis of earthquake soils and structures (hundreds of papers).

The basic principles of thermodynamics are frequently used to derive new constitutive models, for example by Dafalias and Popov [18], Ziegler and Wehrli [19], Collins and Houlsby [20], Houlsby and Puzrin [21], Collins [22], Collins and Kelly [23], Collins [24] and Feigenbaum and Dafalias [25]. The concept of plastic free energy is introduced to enforce the second law of

thermodynamics for developed constitutive models. It is important to distinguish between energy dissipation due to plasticity and plastic work, which is often a source of a confusion. Plastic work is the combination of plastic free energy and plastic energy dissipation, which is defined as the amount of heat (and other forms of energy) transformed from mechanical energy during an irreversible dissipative process. The physical nature of plastic free energy is illustrated later in this paper through a conceptual example that is analyzed on particle scale. Essentially, development of plastic free energy is caused by particle rearrangement in granular assembly under external loading.

Specific formulation of free energy depends on whether the elastic and plastic behavior of the material is coupled. According to Collins et al. [[20], [22], [24]], material coupling behavior can be divided into modulus coupling, where the instantaneous elastic stiffness (or compliance) moduli depend on the plastic strain, and dissipative coupling, where the rate of dissipation function depends not only on the plastic strains and their rates of change but also on the stresses (or equivalently the elastic strains). The modulus coupling describes the degradation of stiffness as in for rock and concrete, and is usually modeled by employing a coupled elastic–plastic constitutive model or by introducing damage variables. The dissipative coupling is considered to be one of the main reasons for non-associative behavior in geomaterials [[20], [26]].

A number of stability postulates are commonly used to prevent violation of principles of thermodynamics. Stability postulates include Drucker's stability condition [[27], [28]], Hill's stability condition [[29], [30]], and Il'lushin's stability postulate [[31], [32]]. As summarized in a paper by Lade [33], theoretical considerations by Nemat–Nasser [34] and Runesson and Mrŏz [35] have suggested that they are sufficient but not necessary conditions for stability. These stability postulates can indeed ensure the admissibility of the constitutive models by assuming certain restrictions on incremental plastic work. As demonstrated by Collins [22], if the plastic strain rate is replaced by the irreversible stain rate in Drucker's postulate, then all the standard interpretations of the classical theory still apply for coupled materials. Dafalias [36] also modified Il'lushin's postulate in a similar way and applied it to both coupled and uncoupled materials.

It is important to note that development of inelastic deformation in geomaterials involves large changes in entropy, and significant energy dissipation. It is thus useful to perform energy dissipation (balance) analysis for all models with inelastic deformation. In this paper we focus on energy dissipation on material level. Focus is on proper modeling that follows thermodynamics. Comparison is made between accumulated plastic dissipation and accumulated plastic work, since these quantities can be quite different in most cases. As a way of verification, the input work, which is introduced by applying external forces, is compared with the stored energy

and dissipation in the entire system. Finally, conclusions on plastic energy dissipation are drawn from the verified results.

2. Theoretical and computational formulations

2.1. Thermo-mechanical theory

For energy analysis of elastic–plastic materials undergoing isothermal process, it is beneficial to start from the statement of the first and second laws of thermodynamics:

$$\widehat{W} = \dot{\Psi} + \Phi \tag{2}$$

where $\Phi \geq 0$ and $\hat{W} \equiv \sigma : \dot{\epsilon} = \sigma_{ij}\dot{\epsilon}_{ij}$ is the rate of work per unit volume. The function Ψ is the Helmholtz free energy, and Φ is the rate of dissipation; both defined per volume. The free energy Ψ is a function of the state variables (also known as internal variables), but Φ and $\hat{W}$ are not the time derivatives of the state functions. The choice of state variables depends on the complexity of constitutive model that is being used, as cyclic loading with certain hardening behaviors usually requires more state variables. This will be elaborated in the following sections as we discuss specific elastic–plastic material models.

For general elastic–plastic materials, the free energy depends on both the elastic and plastic strains. In most material models, it can be assumed that the free energy Ψ can be decomposed into elastic and plastic parts:

$$\Psi = \Psi_{el} + \Psi_{pl}. \tag{3}$$

The total rate of work associated with the effective stress can be written as the sum of an elastic and plastic component:

$$\widehat{W}^{el} \equiv \sigma_{ij}\dot{\epsilon}^{el}_{ij} = \dot{\Psi}_{el} \tag{4}$$

and

$$\widehat{W}^{pl} \equiv \sigma_{ij}\dot{\epsilon}^{pl}_{ij} = \dot{\Psi}_{pl} + \Phi. \tag{5}$$

Note that the focus of this paper is the energy dissipation caused by material plasticity, which should be distinguished from viscous coupling and other sources of energy dissipation. So the effects of solid–fluid interaction are neglected and all stresses are defined as effective stresses in further derivations. In order to avoid confusion, the common notation (σ_{ij}') will not be used. Standard definition of stress from mechanics of materials, i.e. positive in tension, is used.

In the case of a decoupled material, the elastic free energy Ψel depends only on the elastic strains, and the plastic free energy Ψpl depends only on the plastic strains, as shown by Collins and Houlsby [20]:

$$\Psi = \Psi_{el}\left(\epsilon_{ij}^{el}\right) + \Psi_{pl}\left(\epsilon_{ij}^{pl}\right). \quad (6)$$

The effective stress can also be decomposed into two parts:

$$\sigma_{ij} = \alpha_{ij} + \chi_{ij} \quad (7)$$

where χij is a stress-like variable that is related to the dissipative behavior of elastic–plastic material. The difference between the actual stress σij and the stress-like variable χij is another stress-like term αij, which is defined from the plastic free energy function Ψpl. In simple kinematic hardening models, this variable αij controls the shift behavior of stress under cyclic loading, and thus usually referred to as shift or back stress.

Ziegler's orthogonal postulate [19] ensures the validity of Eq. (7). It is equivalent to the maximum entropy production criterion, which is necessary to obtain unique formulation. Also, this is a weak assumption so that all the major continuum models of thermo-mechanics are included. Eq. (5) of plastic work rate can hence be rewritten as:

$$\widehat{W}^{pl} \equiv \sigma_{ij}\dot{\epsilon}_{ij}^{pl} = \dot{\Psi}_{pl} + \Phi = \alpha_{ij}\dot{\epsilon}_{ij}^{pl} + \chi_{ij}\dot{\epsilon}_{ij}^{pl}. \quad (8)$$

The plastic work Wˆpl is the product of the actual Cauchy stress σij with the plastic strain rate ε̇ijpl, while the dissipation rate Φ is the product of the stress variable χij with the plastic strain rate ε̇ijpl. They are only equal if the rate of plastic free energy Ψpl is zero, or equivalently, if the free energy depends only on the elastic strains.

In kinematic hardening models, where the back stress describes the translation (or rotation) of the yield surface, the decomposition of the true stress (sum of back stress and dissipative stress) is a default assumption. Although such a shift stress is important for anisotropic material models, Collins and Kelly [23] have pointed out that it is also necessary in isotropic models of geomaterials with different strength in tension and compression.

2.2. Plastic free energy

A popular conceptual model, which focused on particulate materials and demonstrated the physical occurrence of shift stresses, was described by Besseling and Van Der Giessen [37]and Collins and Kelly [23]. On macro (continuum) scale, every point in a given element is at yield state and deforms plastically. But on meso-scale, only part of this element is undergoing plastic deformations, the remaining part is still within yield

surface and responds elastically. The elastic strain energy stored in the elastic part of a plastically deformed macro-continuum element is considered to be locked into the macro-deformation, giving rise to the plastic free energy function Ψpl and its associated back stress αij. This energy can be released only when the plastic strains are reversed.

For better explanation, the nature of plastic free energy in particulate materials is illustrated through a finite element simulation combined with considerations of particle rearrangement on mesoscopic scale. Fig. 1 shows stress–strain response of Drucker–Prager with nonlinear Armstrong–Frederick kinematic hardening, a typical elastic–plastic model for metals and geomaterials. Six states during shear are chosen to represent evolution of micro fabric of the numerical sample. Correspondingly, Fig. 2 shows the process of particle rearrangement of the 2D granular assembly under cyclic shearing from microscopic level. The square window can be roughly considered as a representative volume (a constitutive level or a finite element) in FEM.

By discussing movement and energy of particle A in Fig. 2, the physical nature of plastic free energy is illustrated. At state (a), which is the beginning of deformation, particle A does not bear any load other than its self weight. State (b) is in middle of loading, when particle B pushes downwards to particle A until it makes contact with particle D and E. Load reaches peak at state (c), and there is no space for particle A to move. Then the sample is unloaded to state (d). Particle A is now stuck between particles C, D, and F, which means that certain amount of elastic energy is stored due to particle elastic deformation. Compared with state (a), this part of elastic energy is not released when the sample is unloaded, which indicates that it is not classic strain energy. This part of elastic energy on particle level which cannot be released by unloading is defined as the plastic free energy in granular materials. Reverse loading starts at state (e), where particle D pushes particle A upwards, making it squeeze through particle C and F. Elastic energy on particle level, which is now defined as plastic free energy, is released during reverse loading.

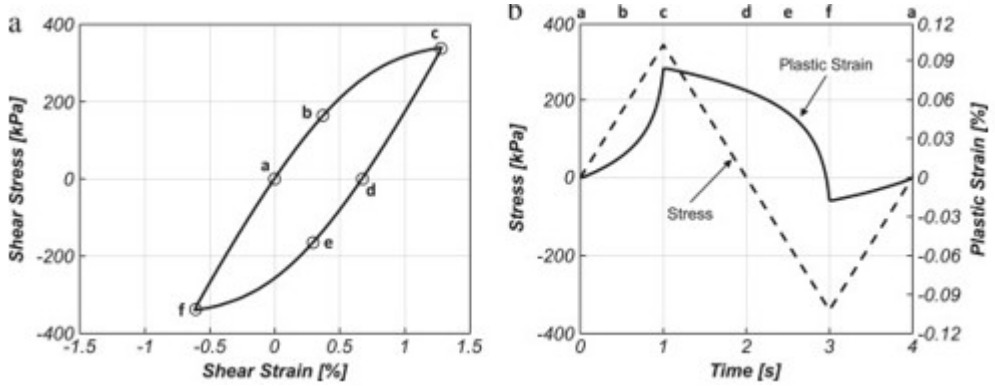

Fig. 1. Elastic–plastic material modeled with Drucker–Prager yield function and Armstrong–Frederick kinematic hardening under cyclic shear loading: (a) Stress–strain curve; (b) stress and plastic strain versus time.

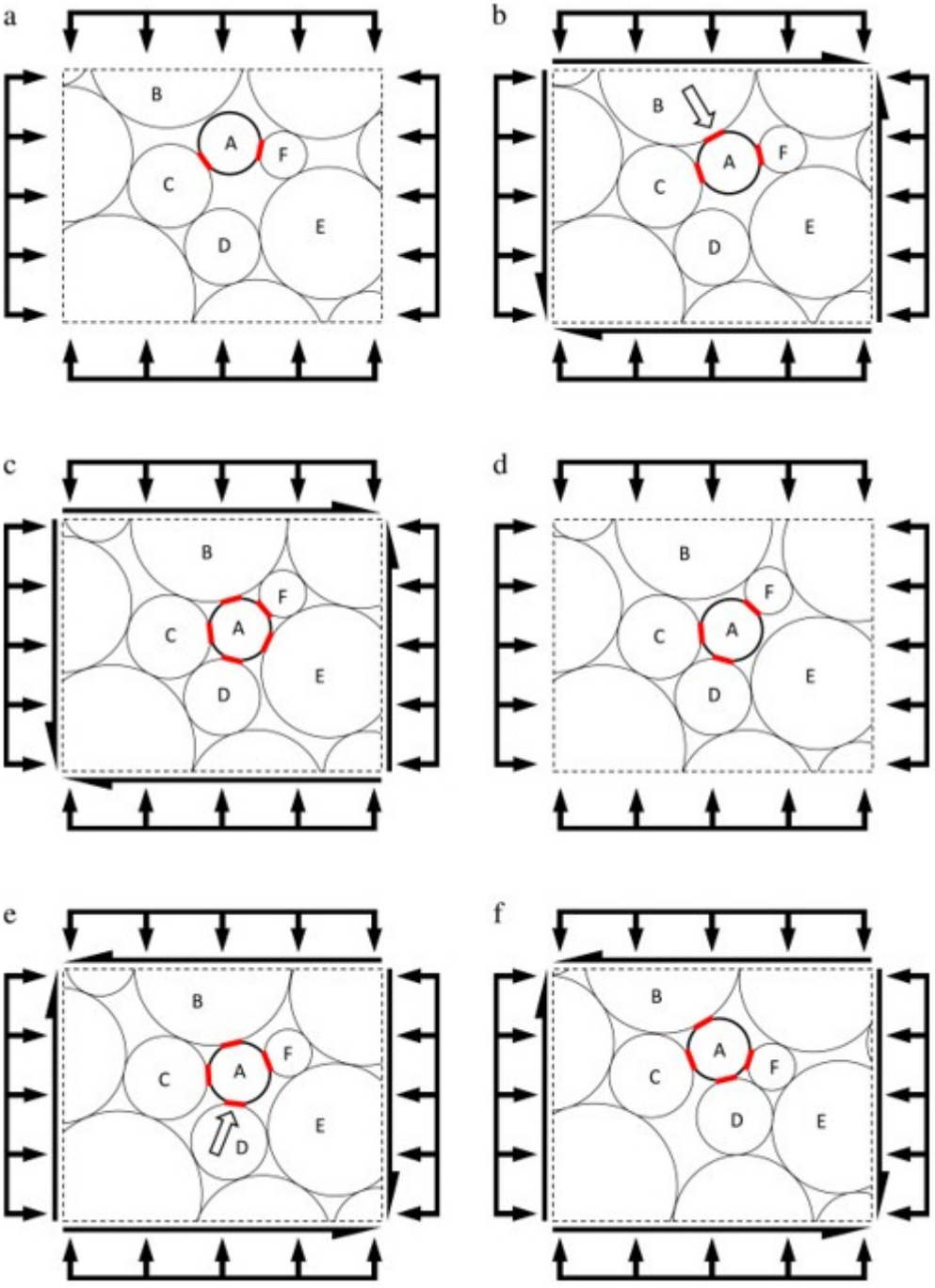

Fig. 2. Particle rearrangement of a 2D granular assembly under cyclic shearing: (a) Initial state; (b) Loading (accumulating plastic free energy); (c) End of loading (maximum plastic free energy); (d) Unloading (plastic free energy unchanged); (e) Reverse loading (releasing plastic free energy); (f) End of reverse loading (plastic free energy released).

By analyzing this example, an explanation on particle scale is provided for the origin of plastic free energy in granular materials. It is important to note

that the concept of plastic free energy also exists in metals and other materials, as studied by Dafalias et al. [38] and Feigenbaum and Dafalias [25]. The physical nature of plastic free energy in these materials can be different and probably should be studied on molecular and/or crystalline level.

Collins [[23], [24]] suggested that in the case of granular materials, the particle-level plastic energy dissipation during normal compaction, arises from the plastic deformations occurring at the inter-granular contacts on the strong force chains, that are bearing the bulk of the applied loads. Collins also suggested that the locked-in elastic energy is produced in the weak force networks, where the local stresses are not large enough to produce plastic deformation at the grain contacts. The plastic strains can be associated with the irreversible rearrangement of the particles, whilst the elastic energy arises from the elastic compression of the particle contacts. Part of this elastic strain energy will be released during unloading, however other part of this energy will be trapped as a result of the irreversible changes in the particle configuration.

2.3. Plastic dissipation

As pointed out, plastic work and energy dissipation are not the same physical quantity. The confusion of these two concepts often leads to incorrect results and conclusions, especially in seismic energy dissipation analysis. Of major concern in this paper is the computation of plastic dissipation, as elaborated in this section.

With the decoupling assumption (Eq. (6)), the second law of thermodynamics (positive entropy production) directly leads to the dissipation inequality, which states that the energy dissipated due to the difference of the plastic work rate and the rate of the plastic part of the free energy must be non-negative:

$$\Phi = \sigma_{ij}\dot{\epsilon}^{pl}_{ij} - \dot{\Psi}_{pl} = \sigma_{ij}\dot{\epsilon}^{pl}_{ij} - \rho\dot{\psi}_{pl} \geq 0 \qquad (9)$$

where ψpl is the rate of plastic free energy, per unit mass, and ρ is the mass density. In addition, ψpl denotes plastic free energy density, which is generally not constant at different locations in a body. This expression is closer to physics and makes it convenient for further derivations.

Now we proceed to consider how to calculate plastic free energy, which can then be used to calculate dissipation. According to Feigenbaum and Dafalias [25], plastic free energy density ψpl is assumed to be additively decomposed into parts which correspond to the isotropic, kinematic and distortional hardening mechanisms as follows:

$$\psi_{pl} = \psi^{iso}_{pl} + \psi^{ani}_{pl}; \quad \psi^{ani}_{pl} = \psi^{kin}_{pl} - \psi^{dis}_{pl} \qquad (10)$$

where ψpliso, ψplani, ψplkin, and ψpldis are the isotropic, anisotropic, kinematic, and distortional parts of the plastic free energy, respectively. The anisotropic part is assumed to decompose into kinematic and distortional parts, which correspond to different hardening models. The subtraction, instead of addition, of ψpldis from ψplkin, to obtain the overall anisotropic part ψplaniof the plastic free energy, is a new concept proposed by Feigenbaum and Dafalias [25]. This expression can better fit experimental data, as well as satisfy the plausible expectations for a limitation of anisotropy development. The distortional part of the plastic free energy ψpldis is related to the directional distortion of yield surface and will only be present if the material model incorporates distortional strain hardening, which is not considered in the formulations and examples of this study.

As pointed out by Dafalias et al. [38], the thermodynamic conjugates to each of the internal variables exist and each part of the plastic free energy can be assumed to be only a function of these conjugates. The explicit expressions for the isotropic and kinematic components of the plastic free energy are:

$$\psi_{pl}^{iso} = \psi_{pl}^{iso}\left(\bar{k}\right) = \frac{\kappa_1}{2\rho}\bar{k}^2; \quad \psi_{pl}^{kin} = \psi_{pl}^{kin}\left(\bar{\alpha}_{ij}\right) = \frac{a_1}{2\rho}\bar{\alpha}_{ij}\bar{\alpha}_{ij} \qquad (11)$$

where k̄ and ᾱij are the thermodynamic conjugates to k (size of the yield surface) and αij(deviatoric back stress tensor representing the center of the yield surface), respectively. Material constants κ1 and a1 are non-negative material constants whose values depend on the choice of elastic–plastic material models.

According to definition, the thermodynamic conjugates are related to the corresponding internal variables by:

$$k = \rho\frac{\partial\psi_{pl}^{iso}}{\partial\bar{k}} = \kappa_1\bar{k}; \quad \alpha_{ij} = \rho\frac{\partial\psi_{pl}^{kin}}{\partial\bar{\alpha}_{ij}} = a_1\bar{\alpha}_{ij}. \qquad (12)$$

By substituting Eq. (12) back into Eq. (11), the plastic free energy can be expressed in terms of the internal variables:

$$\psi_{pl}^{iso} = \frac{1}{2\rho\kappa_1}k^2; \quad \psi_{pl}^{kin} = \frac{1}{2\rho a_1}\alpha_{ij}\alpha_{ij}. \qquad (13)$$

With Eq. (13), the components of plastic free energy can be computed, as long as the internal variables are provided. Combining Eq. (9) with (13), the plastic dissipation in a given elastic–plastic material can be accurately obtained at any location, at any time. This approach allows engineers and designers to correctly identify energy dissipation in time and space and make appropriate conclusions on material behavior.

2.4. Energy computation in finite elements

Formulations from the previous section are applied to FEM analysis in order to follow energy dissipation. Energy density is chosen as the physical parameter for energy analysis. Energy density in this study is defined as the amount of energy stored in a given region of space per unit volume.

For FEM simulations, both external forces and displacements can be prescribed. The finite element program accepts either (or both) forces and/or displacements as input and solves for the other. Either way, the rate of input work can be calculated by simply multiplying force and displacement within a time step. Therefor input work of a finite element model is:

$$W_{Input}(t) = \int_0^t \dot{W}_{Input}(T)\,dT = \int_0^t \sum_i F_i^{ex}(\boldsymbol{x},T)\,\dot{u}_i(\boldsymbol{x},T)\,dT \tag{14}$$

where Fiex is the external force and ui is the displacement computed at the location of the applied load, at given time step, for a load controlled analysis. The external load can have many forms, including nodal loads, surface loads, and body loads. All of them are ultimately transformed into nodal forces. As shown in Eq. (14), input work is computed incrementally at each time step, in order to obtain the evolution of total input work at certain time.

As shown in Fig. 3, when loads and/or displacements are introduced into a finite element model, the input energy will be converted in a number of different forms as it propagates through the system. Input energy will be converted into kinetic energy, free energy, and dissipation. As mentioned before, free energy can be further separated into elastic part, which is traditionally defined as strain energy, and plastic part, which is defined as the plastic free energy. Kinetic energy and strain energy can be considered as the recoverable portion of the total energy since they are transforming from one to another. Plastic free energy is more complicated in the sense that it is conditionally recoverable during reverse loading, as has been discussed in detail in previous sections. Other than kinetic energy and free energy, the rest of the input energy is dissipated, transformed into heat or other forms of energy that are irrecoverable.

Calculation of kinetic energy and strain energy is rather straight forward:

$$U_K(\boldsymbol{x},t) = \tfrac{1}{2}\rho \dot{u}_{ij}(\boldsymbol{x},t)\,\dot{u}_{ij}(\boldsymbol{x},t) \tag{15}$$

$$U_S(\boldsymbol{x},t) = \int_0^t \dot{U}_S(\boldsymbol{x},T)\,dT = \int_0^t \sigma_{ij}(\boldsymbol{x},T)\,\dot{\epsilon}_{ij}^{el}(\boldsymbol{x},T)\,dT \tag{16}$$

where UK and US are the kinetic energy density and strain energy density, respectively.

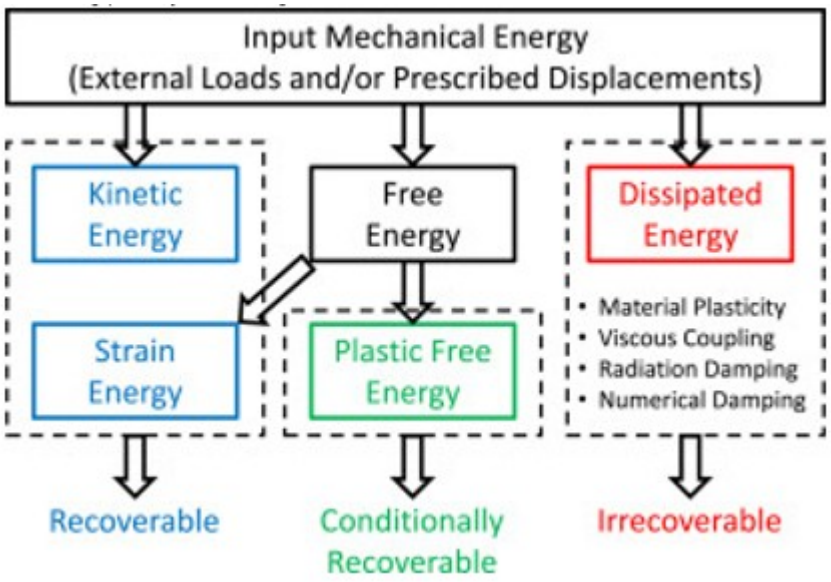

Fig. 3. Different forms of energy in a dynamic soil-structure system.

Similar to the input energy, strain energy density and plastic free energy are also computed incrementally. Integrating energy density over the entire model, corresponding energy quantities are expressed as:

$$E_K(t) = \int_V U_K(\boldsymbol{x}, t)\, dV \tag{17}$$

$$E_S(t) = \int_V U_S(\boldsymbol{x}, t)\, dV \tag{18}$$

$$E_P(t) = \int_V \Psi_{pl}(\boldsymbol{x}, t)\, dV \tag{19}$$

where EK, ES, and EP are the kinetic energy, strain energy, and plastic free energy of the entire model, respectively. Energy densities, defined in Eqs. (15), (16) are functions of both time and space, while energy components, defined in the above equations (Eqs. (17), (18), (19)) are only functions of time, since they are integrated over the whole model.

Although the plastic free energy is conditionally recoverable, it is still considered to be stored in the system, rather than dissipated. Summing up all the stored energy EStored, one obtains:

$$E_{Stored} = E_K + E_S + E_P. \tag{20}$$

Rate of plastic dissipation, given by Eq. (9), can be integrated over time and space:

$$D_P(t) = \int_V \int_0^t \Phi(\boldsymbol{x}, T)\, dT dV \tag{21}$$

where DP is the dissipation due to plasticity of the entire model at certain time.

Finally the energy balance of a finite element model is given by:

$$W_{Input} = E_{Stored} + D_P = E_K + E_S + E_P + D_P. \qquad (22)$$

3. Numerical studies

Numerical simulation results presented in this paper are performed using the Real ESSI (Real Earthquake Soil Structure Interaction) Simulator [39]. Examples in this paper focus on constitutive behavior of elastic–plastic material from the perspective of energy dissipation.

All cases are assumed to be static problems. External loads are applied incrementally using load- or displacement-control scheme. System equations are solved using Newton–Raphson iteration algorithm and UMFPACK solver. Standard 8-node-brick elements are used in all cases, in order to eliminate the variation in energy computation caused by different element types.

3.1. Elastic material

Initial investigation of energy dissipation is focused on linear elastic material. It is noted that linear elastic material does not dissipate energy. Use of linear elastic material model is suitable for preliminary verification of the newly developed energy analysis methodology. In this section, energy balance in a single brick element and a cantilever beam is studied, as shown in Fig. 4.

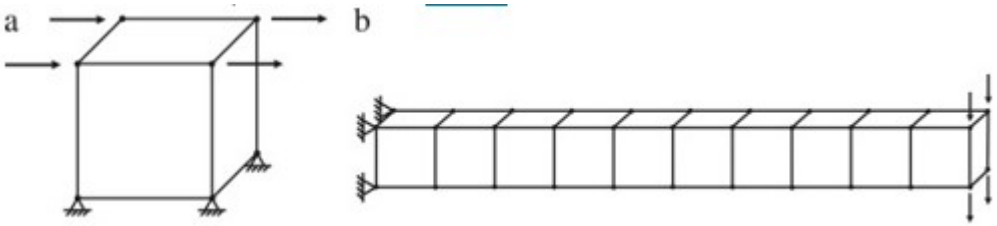

Fig. 4. Numerical models used in this paper: (a) Single brick element; (b) Cantilever with 10 brick elements.

It should be mentioned that the bending deformations of cantilever are not accurate due to the use of a single layer of 8-node-brick elements in the direction of stress and strain variation. However, the focus of this example is energy transformation and balance, which are not affected by inaccurate deformations in this example.

The simplest case is a single element model under uniform shear load. The model is constrained appropriately to simulate simple shear test. In order to show the influence of different material parameters and loads, a set of simulations are performed and the results are presented in Table 1 and Fig. 5.

Since linear elastic material is used with static algorithm, energy components related to dynamics (kinetic energy) and plasticity (plastic free energy and plastic dissipation) are equal to zero. This means that all input work is stored in the system, as observed in all cases.

Table 1. Energy analysis results for linear elastic materials (single element).

Material property		**Simulation results**						
E **(GPa)**	ν	u **(m)**	WInput **(J)**	EK **(J)**	ES **(J)**	EP **(J)**	EStored **(J)**	DP **(J)**
100	**0.30**	**2.60E−5**	**13.00**	**0.00**	**13.00**	**0.00**	**13.00**	**0.00**
150	0.30	1.73E−5	8.67	0.00	8.67	0.00	8.67	0.00
200	0.30	1.30E−5	6.50	0.00	6.50	0.00	6.50	0.00
250	0.30	1.04E−5	5.20	0.00	5.20	0.00	5.20	0.00
300	0.30	8.67E−6	4.33	0.00	4.33	0.00	4.33	0.00
200	0.20	1.20E−5	6.00	0.00	6.00	0.00	6.00	0.00
200	0.25	1.25E−5	6.25	0.00	6.25	0.00	6.25	0.00
200	0.30	1.30E−5	6.50	0.00	6.50	0.00	6.50	0.00
200	0.35	1.35E−	6.75	0.00	6.75	0.00	6.75	0.00

Material property		**Simulation results**						
E **(GPa)**	ν	u **(m)**	WInput **(J)**	EK **(J)**	ES **(J)**	EP **(J)**	EStored **(J)**	DP **(J)**
200	0.40	5 1.40E−5	7.00	0.00	7.00	0.00	7.00	0.00

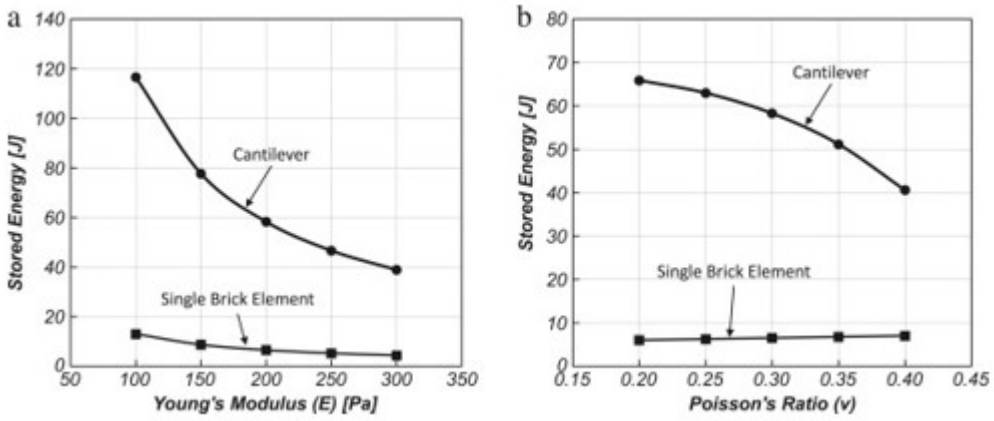

Fig. 5. Relationships between energy storage and different simulation parameters (single element model): (a) Young's modulus; (b) Poisson's ratio.

Fig. 5 shows that energy stored in the system is inversely proportional to Young's moduli Eand proportional to one plus Poisson's ratio (1+ν). This is expected because of the following equations for strain energy under static shear loading:

$$E_S = \frac{1}{2}\tau\gamma = \frac{1}{2G}\tau^2 = \frac{1+\nu}{E}\tau^2. \quad (23)$$

Note that these relationships are only valid at constitutive level. For models with more finite elements, stress and strain are generally not uniform. The computation of energy depends on the distribution of energy density, and nonuniform stress/strain distribution will result in nonuniform energy density distribution.

In order to study the influence of simulation parameters in larger models, another set of simulations with cantilever model (Fig. 4 b) are performed. Vertical loads are applied to the nodes of the free end. In this case, both shearing and bending occur, which means that in general a full 3D state of stress and strain is present. The results are presented in Table 2and Fig. 5. As expected, energy behavior of cantilever is different than the single-element/constitutive example.

For all cases, the energy balance between input and storage is maintained, which gives us confidence on the energy calculation methodology for elastic material. According to results in Fig. 5, energy stored in the system is still inversely proportional to Young's modulus. This is because the general equation for elastic strain energy density is:

$$E_S = \frac{1}{2E}\left(\sigma_{xx}^2 + \sigma_{yy}^2 + \sigma_{zz}^2 + 2\left(1+\nu\right)\left(\sigma_{xy}^2 + \sigma_{yz}^2 + \sigma_{zx}^2\right)\right). \quad (24)$$

Table 2. Energy analysis results for linear elastic materials (cantilever model).

Material property		**Simulation results**						
E **(GPa)**	ν	u **(m)**	WInput **(J)**	EK **(J)**	ES **(J)**	EP **(J)**	EStored **(J)**	DP **(J)**
100	**0.30**	**2.33E−3**	**116.57**	**0.00**	**116.57**	**0.00**	**116.57**	**0.00**
150	0.30	1.55E−3	77.71	0.00	77.71	0.00	77.71	0.00
200	0.30	1.17E−3	58.28	0.00	58.28	0.00	58.28	0.00
250	0.30	9.33E−4	46.63	0.00	46.63	0.00	46.63	0.00
300	0.30	7.77E−4	38.86	0.00	38.86	0.00	38.86	0.00
200	0.20	1.20E−5	65.89	0.00	65.89	0.00	65.89	0.00
200	0.25	1.26E−3	62.97	0.00	62.97	0.00	62.97	0.00
200	0.30	1.17E−3	58.28	0.00	58.28	0.00	58.28	0.00
200	0.35	1.02E−	51.17	0.00	51.17	0.00	51.17	0.00

Material property		**Simulation results**						
E **(GPa)**	ν	u **(m)**	WInput **(J)**	EK **(J)**	ES **(J)**	EP **(J)**	EStored **(J)**	DP **(J)**
200	0.40	3 8.12E−4	40.60	0.00	40.60	0.00	40.60	0.00

So as long as all the elements have the same Young’s modulus, the relationship between stored energy and Young’s modulus will remain valid.

3.2. von Mises plasticity

Elastic–plastic modeling using von Mises material model has been proven to be effective in modeling pressure-independent materials like steel or other metals. In this section, the energy behavior of models using von Mises plasticity with various hardening rules are examined using the proposed method. The material model parameters used in this section are summarized in Table 3.

Note that associated plasticity is used in all models in this section, which means that the plastic flow direction mij is equal to the gradient of the yield surface nij(=∂f/∂σij). Since the yield function is of von Mises type, associated plasticity leads to the result that only deviatoric plastic flow will appear in all cases.

Table 3. Model parameters for cases using von Mises plasticity.

Parameter	**Unit**	**Hardening type**			
		No hardening	**Linear isotropic**	**Linear kinematic**	**A–F kinematic**
mass_density	**kg/m^3**	**8050**	**8050**	**8050**	**8050**
elastic_modulus	GPa	200	200	200	200
poisson_ratio		0.3	0.3	0.3	0.3
von_mises_radius	MPa	250	250	250	250
isotropic_hardening_rate	GPa		20	0	
kinematic_hardening_rate	GPa		0	50	
armstrong_frederick_ha	GPa				200
armstrong_frederick_cr					100

3.2.1. No hardening (elastic-perfectly plastic)

In this example, elastic-perfectly plastic material is used.
Eqs. (9), (13) indicate that in the case of no hardening the rate of plastic free energy is zero. Then the incremental plastic work is equal to incremental plastic dissipation. Note that this is one of the rare cases where plastic dissipation equals plastic work.

Fig. 6 shows stress–strain curve (left) and energy calculated for elastic-perfectly plastic constitutive model (right) used here.

In this case, the plastic dissipation is equal to the plastic work. This means that the plastic free energy does not develop at all during loading and unloading. Zero plastic free energy points out the absence of fabric evolution of a particulate, elastic–plastic material, as all the input work is dissipated through particle to particle friction. Since there is no plastic free energy EP in this case, the stored energy equals mechanical energy, which is the combination of strain energy ES and kinetic energy EK. Total stored energy EStoreddevelops nonlinearly and always has the same value at the beginning of every loop after the first one. Plastic dissipation DP increases linearly when the material yields. This can be explained by rewriting Eq. (9) with Ψpl=0:

$$\dot{\Psi}_{pl} = 0:$$

$$\dot{\Phi} = \sigma_{ij}\dot{\epsilon}_{ij}^{pl} \qquad (25)$$

where stress σij is constant after elastic perfectly plastic material yields, and rate plastic deformation ε̇ijpl is also constant. Then the rate of plastic dissipation is constant which makes the plastic dissipation DP increase linearly.

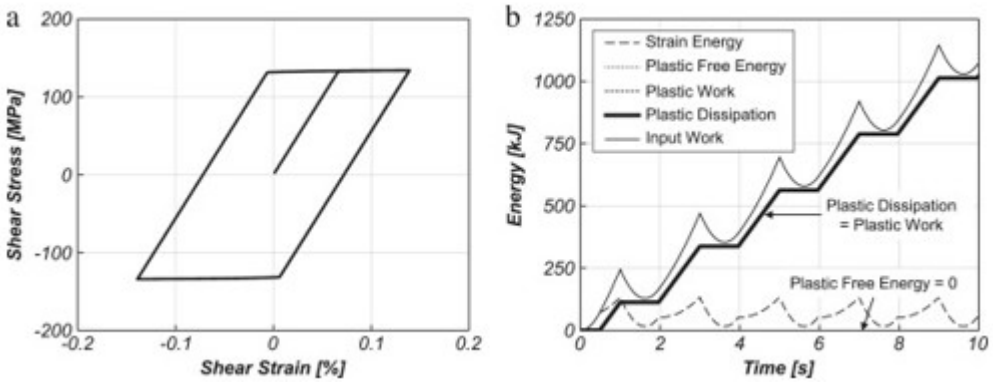

Fig. 6. Energy analysis of elastic–plastic material modeled using von Mises plasticity with no hardening: (a) Stress–strain curve; (b) Input work, plastic dissipation, strain energy and plastic work.

3.2.2. Linear isotropic hardening

Next material model used is von Mises plasticity with linear isotropic hardening. First used to model monotonic behavior of elastic–plastic

materials, isotropic hardening assumes that the yield surface maintains shape, while isotropically (proportionally) changing its size. Fig. 7illustrates the stress–strain response as well as energy balance for elastic–plastic material with isotropic hardening.

As can be observed from Fig. 7, plastic free energy is equal to the plastic work, which means that the plastic dissipation is zero during cycles of loading. Even though this might sound surprising, it can be explained using basic thermodynamics. Linear isotropic hardening, used in this case, can be described through a rate of the internal variable (size of the yield surface) k̇ as:

$$\dot{k} = \kappa_1 \left| \dot{\epsilon}_{ij}^{pl} \right| \tag{26}$$

where |ε̇ijpl| is the magnitude of the rate of plastic strain while κ1 is a hardening constant. The hardening constant κ1 is denoted as isotropic_hardening_rate in Table 3. Substituting previous equation into Eq. (13) yields:

$$\psi_{pl} = \psi_{pl}^{iso} = \frac{\kappa_1}{2\rho} \epsilon_{ij}^{pl} \epsilon_{ij}^{pl}. \tag{27}$$

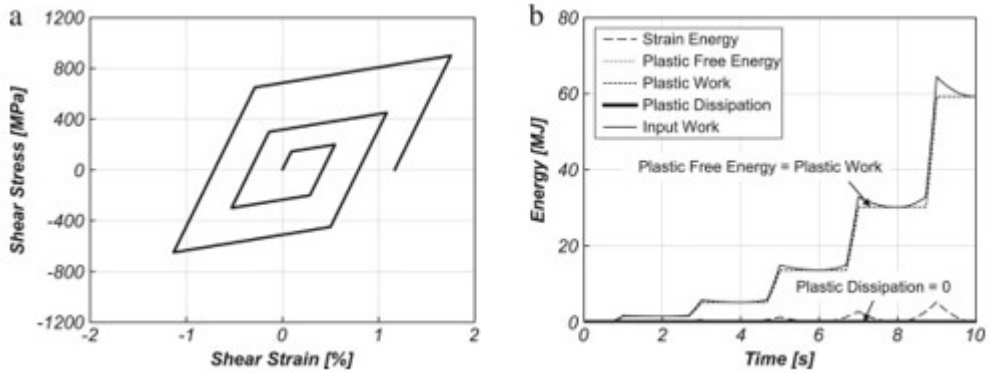

Fig. 7. Energy analysis of elastic–plastic material modeled using von Mises plasticity with linear isotropic hardening: (a) Stress–strain curve; (b) Input work, plastic dissipation, strain energy, and plastic work.

Take the time derivative of the above equation:

$$\dot{\psi}_{pl} = \frac{\kappa_1}{\rho} \epsilon_{ij}^{pl} \dot{\epsilon}_{ij}^{pl}. \tag{28}$$

Then the rate of dissipation due to plasticity can be expressed as:

$$\Phi = \sigma_{ij} \epsilon_{ij}^{pl} - \rho \dot{\psi}_{pl} = \left(\sigma_{ij} - \kappa_1 \epsilon_{ij}^{pl} \right) \dot{\epsilon}_{ij}^{pl} = \left(\sigma_{ij} - k m_{ij} \right) \dot{\epsilon}_{ij}^{pl} \tag{29}$$

where mij is the plastic flow direction. The plastic flow direction defines the direction of incremental plastic strain, which can be different from the

direction of total plastic strain. But in the case of associated von Mises plasticity with only isotropic hardening, the plastic flow direction mij is the same as the direction of the total plastic strain ϵijpl. Thus we have κ1ϵijpl=kmij in the above equation.

Substitute the plastic flow direction mij with the gradient of yield surface nij, and also note that σijε̇ijpl=sijε̇ijpl, where sij(=σij−1/3δijσkk) is the deviatoric part of the stress tensor, the rate of plastic dissipation can be rewritten as:

$$\Phi = (s_{ij} - kn_{ij})\,\dot{\epsilon}_{ij}^{pl} = \alpha_{ij}\dot{\epsilon}_{ij}^{pl}. \tag{30}$$

Realizing that the back stress αij is always zero since we assume no kinematic hardening, then the rate of plastic dissipation becomes zero, which means there is no energy dissipation during cycles of loading for isotropically hardening material. Obviously, the observed response is not physical from the perspective of energy dissipation. Therefore, isotropic hardening material models cannot properly model energy dissipation, even for monotonic loading.

3.2.3. Prager linear kinematic hardening

Compared with isotropic hardening, kinematic hardening can better describe the constitutive, stress–strain behavior of elastic–plastic materials, particularly for cyclic loading. Elastic–plastic material that relies on kinematic hardening is used to analyze energy dissipation. Both linear and nonlinear kinematic hardening rules are investigated in relation to energy dissipation.

Prager's linear kinematic hardening rule is given as:

$$\dot{\alpha}_{ij} = a_1\dot{\epsilon}_{ij}^{pl} \tag{31}$$

where a1 is a hardening constant. The hardening constant a1 is denoted as kinematic_hardening_rate in Table 3.

If only linear kinematic hardening (Eq. (31)) is assumed, the back stress αij is expressed explicitly, and can be substituted into Eq. (13) yielding:

$$\psi_{pl} = \psi_{pl}^{kin} = \frac{a_1}{2\rho}\epsilon_{ij}^{pl}\epsilon_{ij}^{pl}. \tag{32}$$

Take the time derivative of the above equation:

$$\dot{\psi}_{pl} = \frac{a_1}{\rho}\epsilon_{ij}^{pl}\dot{\epsilon}_{ij}^{pl}. \tag{33}$$

Then the rate of dissipation due to plasticity can be rewritten as:

$$\Phi = \sigma_{ij}\dot{\epsilon}_{ij}^{pl} - \rho\dot{\psi}_{pl} = (s_{ij} - \alpha_{ij})\,\dot{\epsilon}_{ij}^{pl} = km_{ij}\dot{\epsilon}_{ij}^{pl} \tag{34}$$

Notice that the term mijėijpl denotes the magnitude of the rate of plastic strain. Since only linear kinematic hardening is assumed, the internal variable k will remain constant. So if loads are applied in such a way that the rate of plastic strain is constant, then the rate of dissipation will also remain constant. In other words, the accumulated dissipation will be linearly increasing under the assumption of linear kinematic hardening.

Fig. 8 shows stress–strain response (left) and energy computation results (right) of an elastic–plastic material modeled using von Mises plasticity with linear kinematic hardening.

As expected, the plastic dissipation increases linearly once the material yields. In contrast to the isotropic hardening case, a significant amount of the input work is dissipated due to material plasticity. The ratio of dissipated energy to input work is largely influenced by the material parameters. However, in general, energy dissipation will be observed if kinematic hardening model is used.

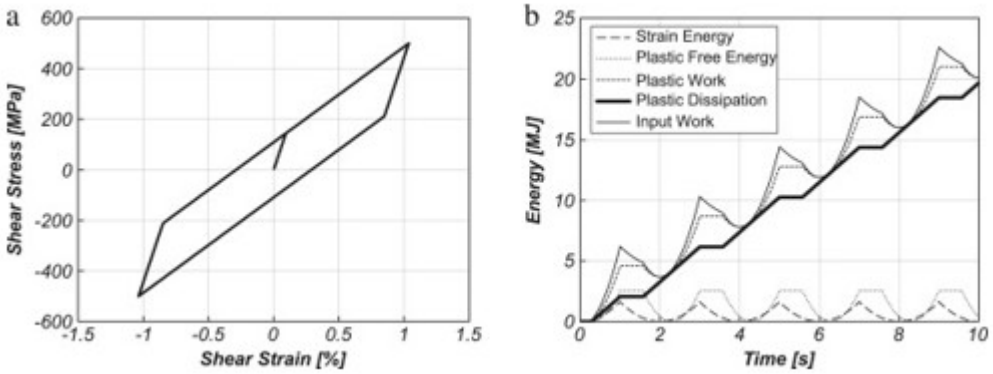

Fig. 8. Energy analysis of elastic–plastic material modeled using von Mises plasticity with linear kinematic hardening: (a) Stress–strain curve; (b) Input work, plastic dissipation strain energy and plastic work.

Another important observation is that the plastic work decreases during certain phases of reverse loading, while the actual rate of energy dissipation is always nonnegative. It is important to distinguish plastic work from plastic energy dissipation. Otherwise, one might argue that accumulated energy dissipation can increase or decrease, which is a common mistake observed in a number of publications that violates the second law of thermodynamics.

3.2.4. Armstrong–Frederick kinematic hardening

Armstrong–Frederick kinematic hardening model [40] is often used to simulate elastic–plastic material behavior under cyclic loading. Material parameters of the Armstrong–Frederick kinematic hardening rule can be derived from basic thermodynamics. The following equation is a general expression for Armstrong–Frederick kinematic hardening rule:

$$\dot{\alpha}_{ij} = a_1 \dot{\epsilon}^{pl}_{ij} - a_2 \dot{\lambda} \alpha_{ij} \qquad (35)$$

where λ̇ is a non-negative scalar plastic multiplier and a2 is a non-negative material hardening constant. It can be proven that a1/a2 is related to the limit of back stress magnitude |αij|. In Table 3, the hardening constants a1 and a2 correspond to parameters armstrong_frederick_ha and armstrong_frederick_cr.

Taking the time derivative of the kinematic part of plastic free energy (Eq. (33)), and substituting the expression of back stress αij (Eq. (35)) gives:

$$\dot{\psi}_{pl}^{kin} = \frac{1}{\rho a_1}\alpha_{ij}\dot{\alpha}_{ij} = \frac{1}{\rho}\alpha_{ij}\left(\dot{\epsilon}_{ij}^{pl} - \frac{a_2}{a_1}\dot{\lambda}\alpha_{ij}\right). \tag{36}$$

Then the rate of plastic energy dissipation of an Armstrong–Frederickkinematic hardening elastic–plastic material is given by:

$$\Phi = \sigma_{ij}\dot{\epsilon}_{ij}^{pl} - \rho\dot{\psi}_{pl} = s_{ij}\dot{\epsilon}_{ij}^{pl} - \alpha_{ij}\dot{\epsilon}_{ij}^{pl} + \frac{a_2}{a_1}\dot{\lambda}\alpha_{ij}\alpha_{ij} = km_{ij}\dot{\epsilon}_{ij}^{pl} + \frac{a_2}{a_1}\dot{\lambda}\alpha_{ij}\alpha_{ij}. \tag{37}$$

Compared with Eq. (34), the above expression has an additional term which makes the rate of plastic dissipation non-constant even if the rate of plastic strain is constant. As the back stress αij becomes larger when load increases, the rate of plastic dissipation also increases. This indicates a nonlinear result of total plastic dissipation, which is exactly what we have observed in our computations.

Fig. 9 shows the energy computation results of an elastic–plastic material modeled using von Mises plasticity with Armstrong–Frederick kinematic hardening. Compared to all previous cases, the material response of this model is more sophisticated and more realistic. Decrease of plastic work is observed, again, while the plastic dissipation is always nonnegative during the entire simulation. For both linear and nonlinear kinematic hardening cases, the plastic free energy is relatively small compared to the plastic dissipation.

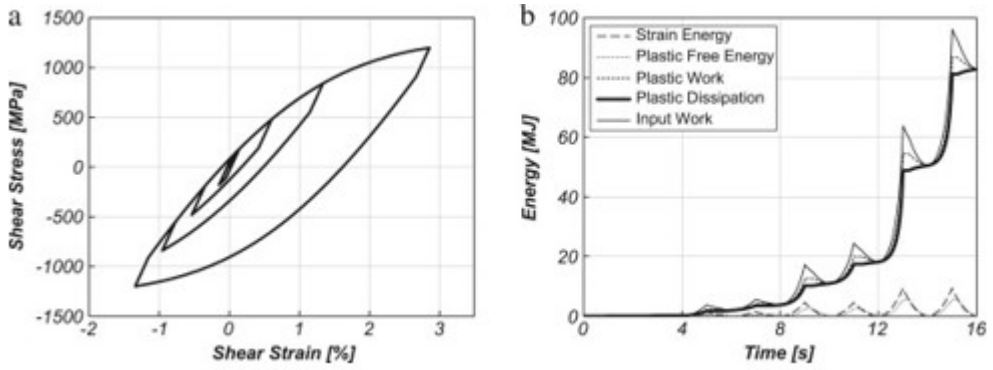

Fig. 9. Energy analysis of elastic–plastic material modeled using von Mises plasticity with Armstrong–Frederick kinematic hardening: (a) Stress–strain curve; (b) Input work, plastic dissipation, strain energy, and plastic work.

3.3. Drucker–Prager plasticity

It has been proven that von Mises plasticity generally performs poorly in modeling pressure-sensitive materials like soils. In this section, the thermomechanical formulations presented in earlier sections are applied to models using Drucker–Prager yield criteria with different hardening types. The material model parameters used in this section are summarized in Table 4.

The yield function of Drucker–Prager plasticity is:

$$f = \left[\left(s_{ij} - p\alpha_{ij}\right)\left(s_{ij} - p\alpha_{ij}\right)\right]^{0.5} - \sqrt{\tfrac{2}{3}}kp \qquad (38)$$

where p=(1/3)δijσkk is the mean stress (or hydrostatic pressure). Note that in this form of Drucker–Prager plasticity, the internal variables αij and k, as well as the hardening constants κ1 and a1, are dimensionless.

Table 4. Model parameters for cases using Drucker–Prager plasticity.

Parameter	**Unit**	**Hardening type**				
		Linear isotropic	**Linear kinematic**	**A–F kinematic**		
mass_density	**kg/m³**	**2000**	**2000**	**2000**	**2000**	**2000**
elastic_modulus	MPa	150	150	200	200	200
poisson_ratio		0.3	0.3	0.3	0.3	0.3
druckerprager_k		0.25	0.5	0.1	0.1	0.1
confining_stress	kPa	100	100	100	300	500
isotropic_hardening_rate		50	0			
kinematic_hardening_rate		0	50			
armstrong_frederick_ha	MPa			20	20	20
armstrong_frederick_cr				100	100	100

For the computation of plastic free energy in Drucker–Prager plasticity models, Eq. (13) is modified:

$$\psi_{pl}^{iso} = \frac{1}{2\rho(\kappa_1 p)}(kp)^2 = \frac{1}{2\rho\kappa_1}k^2 p \tag{39}$$

$$\psi_{pl}^{kin} = \frac{1}{2\rho(a_1 p)}(\alpha_{ij} p)(\alpha_{ij} p) = \frac{1}{2\rho a_1}\alpha_{ij}\alpha_{ij} p. \tag{40}$$

All examples presented in this section are using non-associated Drucker–Prager plasticity. The plastic potential function is of von Mises type so that only deviatoric plastic flow exists. In addition, all cases are loaded with constant hydrostatic pressure, which means that the plastic flow direction mij is the same as the direction of the total plastic strain ϵijpl. With the above conditions, Eqs. (25), (30), (34) are all still valid for the following examples, as will be observed in their results.

It should be noted that the proposed energy computation approach can also be applied to associated Drucker–Prager plasticity and non-associated Drucker–Prager plasticity with different plastic potential functions. The loading condition can be arbitrary, even with evolving hydrostatic pressures. Due to the length limitation of the paper, these topics will be discussed in further publications.

3.3.1. Linear isotropic hardening

Fig. 10 shows the stress–strain response and energy computation results of an elastic–plastic material modeled using Drucker–Prager plasticity with linear kinematic hardening.

No plastic dissipation is observed in this case, which has been theoretically proven in Eq. (30). This example again indicates that isotropic hardening is not capable of proper modeling of energy dissipation in elastic–plastic materials.

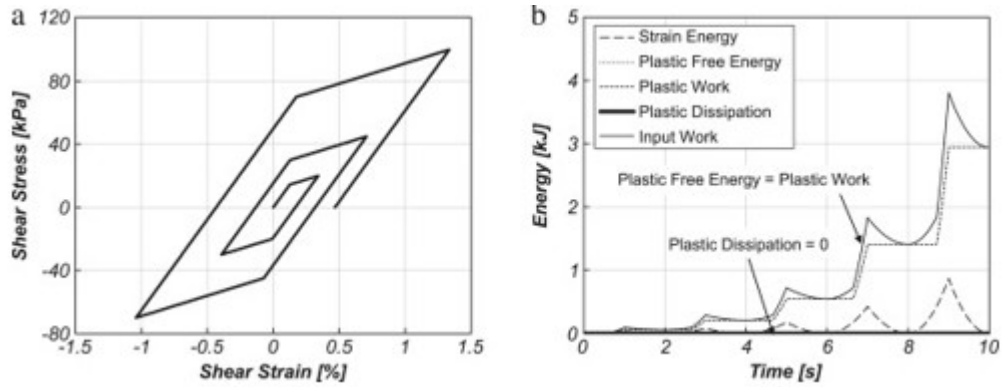

Fig. 10. Energy analysis of elastic–plastic material modeled using Drucker–Prager plasticity with linear isotropic hardening: (a) Stress–strain curve; (b) Input work, plastic dissipation strain energy and plastic work.

3.3.2. Prager linear kinematic hardening

Fig. 11 shows the stress–strain response and energy computation results of an elastic–plastic material modeled using Drucker–Prager plasticity with linear kinematic hardening.

Plastic dissipation increases linearly when the material yields, while the plastic work decreases during certain phases of reverse loading. This observation is consistent with the theoretical conclusion drawn from Eq. (34).

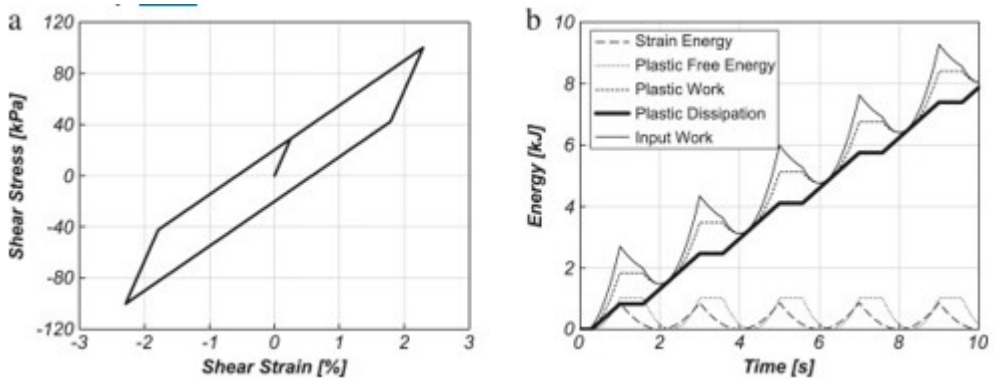

Fig. 11. Energy analysis of elastic–plastic material modeled using Drucker–Prager plasticity with linear kinematic hardening: (a) Stress–strain curve; (b) Input work, plastic dissipation strain energy and plastic work.

Note that the results of the above two examples share high similarity with those of the cases modeled with associated von Mises plasticity. This is because the hydrostatic pressures were constant during shearing, which makes the pressure-dependent feature of Drucker–Prager plasticity not observed. The energy computation results are expected to be more complicated with different loading conditions. However, the difference between plastic work and plastic dissipation will be observed. And the incremental plastic dissipation should always be nonnegative.

3.3.3. Armstrong–Frederick kinematic hardening

In order to illustrate the influence of hydrostatic pressure to the energy dissipation in Drucker–Prager models, three cases with different confining pressures are studied. Armstrong–Frederick kinematic hardening is used here to model the nonlinear hardening response of pressure-dependent material, like soils. Fig. 12 shows the stress–strain response and energy computation results of these three cases.

As can be observed from Fig. 12, the slope of stress–strain loop increases, which means the material becomes stiffer, as the confining stress increases. Also, the size of elastic region becomes larger when the confining stress is bigger.

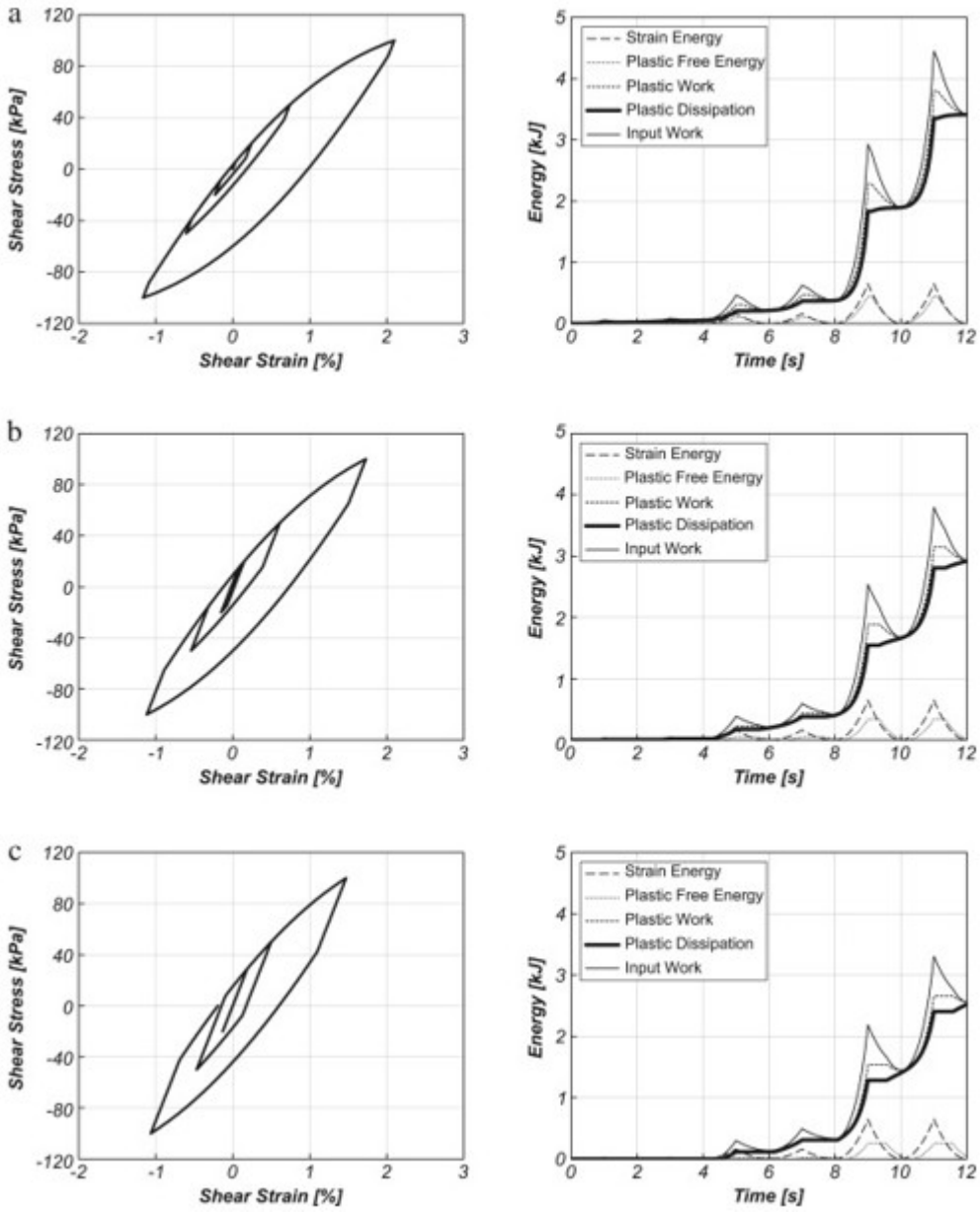

Fig. 12. Energy analysis of elastic–plastic material modeled using Drucker–Prager plasticity with Armstrong–Frederick kinematic hardening: (a) Confining stress = 100 kPa; (b) Confining stress = 300 kPa; (c) Confining stress = 500 kPa.

Plastic dissipation and plastic free energy start to evolve as soon as the material yields. The pattern of evolution of energy components is the same for all three cases, while the value of plastic dissipation decreases as the confining stress increases. This is expected since the material becomes stiffer and harder to plastify with a higher confining stress.

4. Conclusions

Presented was a methodology for (correct) computation of energy dissipation in elastic–plastic materials based on the second law of thermodynamics. A

very important role of plastic free energy was analyzed, with highlights on its physical nature and theoretical formulations. The proposed methodology has been illustrated using a number of elasto-plastic material models.

An analysis of a common misconception that equates plastic work and dissipation, which leads to the violation of the basic principles of thermodynamics, was addressed. A conceptual example, for granular materials, was used to explain the physical meaning of plastic free energy. It was also shown that plastic free energy is responsible for the evolution of internal variables.

It was shown that energy balance is ensured by taking into consideration all energy components, including kinetic and strain energy. Input work was balanced with the stored and dissipated energy, expressed as the summation of all possible components.

Presented approach was illustrated and tested using several elastic–plastic constitutive models with various hardening rules. Elastic materials showed no energy dissipation (as expected), leading to the input work being equal to the stored energy. Elastic-perfectly plastic materials had no change in plastic free energy, which led to the equality of plastic work and plastic dissipation and indicated no evolution of particle arrangements. The plastic dissipation, in that case, was observed to be increasing linearly. Isotropic hardening materials experienced zero dissipation even after yielding. This observation was surprising, but verified by further derivation of energy equations. This observation also serves as a reminder that the isotropic hardening rules can be used, but only with observed lack of energy dissipation. Prager’s linear and Armstrong–Frederick nonlinear kinematic hardening materials both gave significant dissipations, with large fluctuation of plastic free energy as well. In the case with linear kinematic hardening, linear increase of dissipation was derived and observed, while energy was dissipated nonlinearly in the case of nonlinear kinematic hardening. Although the plastic free energy was not significant for some materials, it is noted that it should always be recognized and considered during energy analysis, so that the basic principles of thermodynamics are maintained.

Acknowledgments

This work was supported by the US-DOE . We would like to thank Professor Yannis Dafalias (UCD and NTUA) for inspiring discussions.

References

[1]

Farren W., Taylor G.**The heat developed during plastic extension of metals**

Proc. R. Soc. Lond. Ser. A Math. Phys. Eng. Sci., 107 (743) (1925), pp. 422-451

[2]

Taylor G.I., Quinney H.**The latent energy remaining in a metal after cold working**

Proc. R. Soc. Lond. Ser. A Math. Phys. Eng. Sci., 143 (849) (1934), pp. 307-326

[3]

Clifton R., Duffy J., Hartley K., Shawki T.**On critical conditions for shear band formation at high strain rates**

Scr. Metall., 18 (5) (1984), pp. 443-448

[4]

Belytschko T., Moran B., Kulkarni M.**On the crucial role of imperfections in quasi-static viscoplastic solutions**

J. Appl. Mech., 58 (1991), pp. 658-665

[5]

Zhou M., Ravichandran G., Rosakis A.**Dynamically propagating shear bands in impact-loaded prenotched plates—ii. Numerical simulations**

J. Mech. Phys. Solids, 44 (6) (1996), pp. 1007-1032

[6]

Dolinski M., Rittel D., Dorogoy A.**Modeling adiabatic shear failure from energy considerations**

J. Mech. Phys. Solids, 58 (11) (2010), pp. 1759-1775

[7]

Ren B., Li S.**Meshfree simulations of plugging failures in high-speed impacts**

Comput. Struct., 88 (15) (2010), pp. 909-923

[8]

Osovski S., Rittel D., Venkert A.**The respective influence of microstructural and thermal softening on adiabatic shear localization**

Mech. Mater., 56 (2013), pp. 11-22

[9]

Rittel D.**An investigation of the heat generated during cyclic loading of two glassy polymers. Part i: Experimental**

Mech. Mater., 32 (3) (2000), pp. 131-147

[10]

Rittel D., Rabin Y.**An investigation of the heat generated during cyclic loading of two glassy polymers. Part ii: Thermal analysis**

Mech. Mater., 32 (3) (2000), pp. 149-159

[11]

Rittel D., Eliash N., Halary J.**Hysteretic heating of modified poly (methylmethacrylate)**

Polymer, 44 (9) (2003), pp. 2817-2822

[12]

Rosakis P., Rosakis A., Ravichandran G., Hodowany J.**A thermodynamic internal variable model for the partition of plastic work into heat and stored energy in metals**

J. Mech. Phys. Solids, 48 (3) (2000), pp. 581-607

[13]

Hodowany J., Ravichandran G., Rosakis A., Rosakis P.**Partition of plastic work into heat and stored energy in metals**

Exp. Mech., 40 (2) (2000), pp. 113-123

[14]

Ravichandran G., Rosakis A.J., Hodowany J., Rosakis P., Furnish M.D., Thadha ni N.N., Horie Y.**On the conversion of plastic work into heat during high-strain-rate deformation**

AIP Conference Proceedings, Vol. 620/1, AIP (2002), pp. 557-562

[15]

Veveakis E., Vardoulakis I., Toro G.D.**Thermoporomechanics of creeping landslides: The 1963 vaiont slide, northern Italy**

J. Geophys. Res. Earth Surf., 112 (F3) (2007)

[16]

Veveakis E., Sulem J., Stefanou I.**Modeling of fault gouges with cosserat continuum mechanics: Influence of thermal pressurization and chemical decomposition as coseismic weakening mechanisms**

J. Struct. Geol., 38 (2012), pp. 254-264

[17]

Uang C.-M., Bertero V.V.**Evaluation of seismic energy in structures**

Earthq. Eng. Struct. Dynam., 19 (1) (1990), pp. 77-90

[18]

Dafalias Y., Popov E.**A model of nonlinearly hardening materials for complex loading**

Acta Mech., 21 (3) (1975), pp. 173-192

[19]

Ziegler H., Wehrli C.**The derivation of constitutive relations from the free energy and the dissipation function**

Adv. Appl. Mech., 25 (1987), pp. 183-238

[20]

Collins I.F., Houlsby G.T.**Application of thermomechanical principles to the modelling of geotechnical materials**

Proc. R. Soc. Lond., 453 (1997), pp. 1975-2001

[21]

Houlsby G., Puzrin A.**A thermomechanical framework for constitutive models for rate-independent dissipative materials**

Int. J. Plast., 16 (9) (2000), pp. 1017-1047

[22]

Collins I.**Associated and non-associated aspects of the constitutive laws for coupled elastic/plastic materials**

Int. J. Geomech., 2 (2) (2002), pp. 259-267

[23]

Collins I., Kelly P.**A thermomechanical analysis of a family of soil models**

Geotechnique, 52 (7) (2002), pp. 507-518

[24]

Collins I.**A systematic procedure for constructing critical state models in three dimensions**

Int. J. Solids Struct., 40 (17) (2003), pp. 4379-4397

[25]

Feigenbaum H.P., Dafalias Y.F.**Directional distortional hardening in metal plasticity within thermodynamics**

Int. J. Solids Struct., 44 (22–23) (2007), pp. 7526-7542

[26]

Ziegler H.**Discussion of some objections to thermomechanical orthogonality**

Ing.-Arch., 50 (3) (1981), pp. 149-164

[27]

Drucker D.C.**On uniqueness in the theory of plasticity**

Quart. Appl. Math. (1956), pp. 35-42

[28]

D.C. Drucker, A definition of stable inelastic material. Technical report, DTIC Document, 1957.

[29]

Bishop J., Hill R.**A theory of the plastic distortion of a polycrystalline aggregate under combined stresses**

London Edinburgh Dublin Phil. Mag. J. Sci., 42 (327) (1951), pp. 414-427

[30]

Hill R.**A general theory of uniqueness and stability in elastic–plastic solids**

J. Mech. Phys. Solids, 6 (3) (1958), pp. 236-249

[31]

Il'Iushin A.**On the postulate of plasticity**

J. Appl. Math. Mech., 25 (3) (1961), pp. 746-752

[32]

Lubliner J.

Plasticity Theory, Macmillan Publishing Company, New York (1990)

[33]

Lade P.V.**Instability, shear banding, and failure in granular materials**

Int. J. Solids Struct., 39 (13) (2002), pp. 3337-3357

[34]

Nemat–Nasser S.**On finite plastic flow of crystalline solids and geomaterials**

J. Appl. Mech., 50 (1983), pp. 1114-1126

[35]

Runesson K., Mrŏz Z.**A note on nonassociated plastic flow rules**

Int. J. Plast., 5 (1989), pp. 639-658

[36]

Dafalias Y.F.**Il'iushin's postulate and resulting thermodynamic conditions on elastic–plastic coupling**

Int. J. Solids Struct., 13 (1977), pp. 239-251

[37]

Besseling J.F., Van De. Giessen E.

Mathematical Modeling of Inelastic Deformation Vol. 5, CRC Press (1994)

[38]

Dafalias Y., Schick D., Tsakmakis C., Hutter K., Baaser H.**A simple model for describing yield surface evolution**

Lecture Note in Applied and Computational Mechanics, Springer (2002), pp. 169-201

[39]

Jeremić B., Jie G., Cheng Z., Tafazzoli N., Tasiopoulou P., Abell F.P.J.A., Watan abe K., Feng Y., SinhaS.K., Behbehani F., Yang H., Wang H.

The Real ESSI Simulator System, University of California, Davis and Lawrence Berkeley National Laboratory (2017)

http://real-essi.info/

[40]

P. Armstrong, C. Frederick, A mathematical representation of the multiaxial bauschinger effect. Technical Report RD/B/N/ 731, C.E.G.B. 1966.